

Research on the Optimization Design of Heliostat Field Based on EB Layout and Particle Swarm Algorithm

Ligen Chen^{1,a}, Shuo Zhang^{1,b}, Hang Yu^{2,c}

¹College of Physics and Energy, Fujian Normal University, Fuzhou City, 350117, China

²College of Mathematics and Statistics, Fujian Normal University, Fuzhou City, 350117, China

^a1392374483@qq.com, ^b1040343516@qq.com, ^c97955021@qq.com

Abstract: This study aims to optimize the design of a heliostat field to achieve maximum annual average power output through geometric analysis and coordinate transformation. The research establishes models for annual average optical efficiency and thermal output power, and employs a grid marking method to calculate shading efficiency. The optimization model is simplified by simulating the EB (Edge of Bubble) layout, and the Particle Swarm Optimization (PSO) algorithm is used to search for optimal layout parameters. The results demonstrate that the optimized heliostat field shows significant improvements in both annual average optical efficiency and thermal output power, providing an effective design optimization strategy for solar thermal power generation technology. Additionally, a grid marking method judgment algorithm based on the plane projection model is proposed to further simplify the calculation of complex shadow areas.

Keywords: Heliostat Field, EB Layout, Particle Swarm Optimization, Optical Efficiency, Thermal Output Power, Grid Marking Method

1. Introduction

The quest for sustainable and clean energy sources has never been more critical, as the world grapples with the environmental and economic challenges posed by climate change and dwindling fossil fuel reserves. Solar thermal power generation, with its potential for harnessing the sun's energy to produce electricity, stands out as a promising solution. Central to this technology are heliostats—mirrors that reflect sunlight onto a central receiver, concentrating the solar energy for efficient conversion into heat and, subsequently, electricity [1, 2].

The efficiency of a solar thermal power plant is heavily dependent on the strategic arrangement of its heliostats. Traditional layouts, while functional, often leave room for optimization in terms of maximizing sunlight capture and minimizing shading effects. This paper delves into the optimization of heliostat field design, focusing on the implementation of the EB layout and Particle Swarm Optimization (PSO) algorithm [3, 4]. These methodologies are employed to enhance the optical efficiency and thermal output power of the heliostat field, which are critical parameters for evaluating the performance of solar thermal systems.

Our approach involves a meticulous geometric analysis and the establishment of a coordinate system that facilitates the calculation of solar angles, atmospheric transmittance, and Direct Normal Irradiance (DNI) [5]. By integrating these factors into a comprehensive model, we are able to simulate the performance of the heliostat field under various conditions. The use of a grid marking method further allows us to accurately assess shading efficiency, a complex variable that significantly impacts the overall efficiency of the system [6]. The Particle Swarm Optimization algorithm is then applied to identify the optimal layout parameters, ensuring that the heliostat field operates at peak efficiency. This study not only contributes to the theoretical understanding of heliostat field optimization but also provides practical insights that can be applied in the design and operation of solar thermal power plants.

2. Optical Efficiency and Thermal Output Simulation

Initially, within the specified geometric parameters of a given location, we have calculated the

average optical efficiency and the average thermal output efficiency per unit area of the heliostat mirror surface over a designated time frame. Formulas for determining the solar azimuth angle, solar altitude angle, atmospheric transmittance, and Direct Normal Irradiance (DNI) have been preliminarily established. The computation of cosine efficiency, truncation efficiency, and shading rate, however, presents greater complexity. To address this, we initially assess the cosine efficiency based on the solar incidence angle. The shading rate and truncation efficiency are then combined within a unified model, with their calculation based on the ratio of light rays before and after the obstruction. Given the difficulty in directly computing the number of light rays, we employ a grid area method to determine the shading efficiency.

2.1. Model Formulation

2.1.1. Coordinate Establishment

Firstly, this paper establishes a coordinate system, with point O set as the point at the same height as the heliostat and the absorption tower. The x-axis points towards the true east direction, the y-axis points towards the true north direction, and the z-axis is perpendicular to the ground, pointing towards the sky. M_n , N_n , P_n , Q_n represent the four vertices of the heliostat, while A_n and B_n respectively represent the direction lines of the incident and reflected sunlight. According to the law of reflection for plane mirrors, it can be deduced that $O_n A_n = O_n B_n$, where $A_n A'_n$ and $C_n C'_n$ are the perpendiculars to the $x-y$ plane. The coordinate diagram is shown in Figure 1.

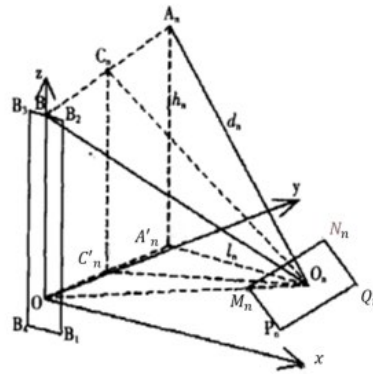


Figure 1: Heliostat field under mirror field coordinate system.

It is also assumed that the coordinate point of the n th mirror is $O_n = (x_n, y_n, 0)$, and any light source coordinate is $A_n = (x'_n, y'_n, h_n)$. It is assumed that the direction vector of the light at this time in the ground coordinate axis is:

$$\vec{V}_0 = (a, b, c) \quad (1)$$

Assuming that the light ray at this time in the mirror coordinate system is \vec{V}_H , and it satisfies the following relationship with vector \vec{V}_0 :

$$\vec{V}_0 = \begin{pmatrix} l_x & l_y & l_z \\ m_x & m_y & m_z \\ n_x & n_y & n_z \end{pmatrix} \cdot \vec{V}_H \quad (2)$$

Where (l_x, m_x, n_x) , (l_y, m_y, n_y) , (l_z, m_z, n_z) are the vector representations of the three axes of the mirror coordinate system a in the ground coordinate system b. Based on the aforementioned conditions, establish the collector coordinate equation:

$$\begin{cases} x^2 + y^2 = \left(\frac{D}{2}\right)^2 \\ h_{tower} - h_{collector} - h_{heliostat} \leq z \leq h_{tower} - h_{collector} \end{cases} \quad (3)$$

2.1.2. Optical Efficiency

Cosine efficiency is an important component in heliostats, which is essentially the cosine of the solar incidence angle. The size of the solar incidence angle is related to the azimuth and altitude angles, as well as the coordinates of the center of the mirror surface. The formula for calculating cosine

efficiency is shown in equation (4):

$$\eta_{cos} = \cos\theta_n = \left(\frac{\sin\alpha_s \cdot H_t + x_n \cos\alpha_s \sin\gamma_s + y_n \cos\alpha_s \cos\gamma_s + d_n}{2d_n} \right)^{\frac{1}{2}} \quad (4)$$

In the formula, H_t represents the distance of OB. The solar altitude angle is:

$$\sin\alpha_s = \cos\delta \cos\phi \cos\omega + \sin\delta \sin\phi \quad (5)$$

The solar azimuth angle is:

$$\cos\gamma_s = \frac{\sin\delta - \sin\alpha_s \sin\phi}{\cos\alpha_s \cos\phi} \quad (6)$$

And the calculation of the solar hour angle is shown in equation (7):

$$\omega = \frac{\pi}{12} (ST - 12) \quad (7)$$

By using the time, solar azimuth angle, and solar altitude angle, the results of the azimuth and altitude angles corresponding to the sun on different dates and how they change over time are determined. Based on the aforementioned formulas, the average cosine efficiency can be obtained:

$$\overline{\eta_{cos}} = \frac{1}{N} \sum_i^N \eta_{icos} \quad (8)$$

Atmospheric transmittance refers to the ratio of the radiation intensity after solar radiation has passed through the atmosphere, affected by atmospheric scattering and absorption by ozone. The calculation formula is shown in equation (9):

$$\eta_{at} = 0.99321 - 0.0001176d_{HR} + 1.97 \times d_{HR}^2 \quad (d_{HR} \leq 1000) \quad (9)$$

Shadow blocking efficiency refers to the loss of energy due to shadow loss, which includes three aspects: 1) The shadow loss caused by the obstruction of the tower in the heliostat field. 2) The loss of sunlight received by the rear heliostats being blocked by the front heliostats. 3) The loss of sunlight emitted by the rear heliostats being blocked by the front heliostats. This paper calculates the shadow loss by determining the ratio of the shadowed area after obstruction to the area without considering obstruction, and thus, the shadow blocking efficiency is obtained.

$$H_1' = \begin{pmatrix} l_x & l_y & l_z \\ m_x & m_y & m_z \\ n_x & n_y & n_z \end{pmatrix}^T \cdot (H_1 - O_m) = \begin{pmatrix} x_{mt}' \\ y_{mt}' \\ z_{mt}' \end{pmatrix} \quad (10)$$

In the equation, O_m represents the coordinates of the origin of the mirror coordinate system m in the ground coordinate system, denoted as (x_m, y_m, z_m) . Based on geometric relationships, the effective utilization rate of sunlight to the heliostat can be calculated as shown in equation (11):

$$\eta_{sn} = \frac{K_s \cdot ds}{\lambda \beta_n} \quad (11)$$

Here, λ denotes the length of the diagonal of the heliostat mirror, β_n represents the angle between the longer side of the mirror and the diagonal, and K_s is the total number of elements that can receive light. Similarly, the effective utilization rate of the heliostat reflecting sunlight to the collector at this time can be calculated as shown in equation (12):

$$\eta_{bn} = \frac{K_b \cdot ds}{\lambda \beta_n} \quad (12)$$

Here, K_b represents the total number of elements that can be reflected onto the collector. In summary, the shadow blocking rate of the heliostat is:

$$\eta_{sb} = 1 - \eta_{sn} * \eta_{bn} \quad (13)$$

Therefore, the average shadow blocking efficiency formula is as shown in equation (14):

$$\overline{\eta_{sb}} = \frac{1}{N} \sum_i^N \eta_{isb} \quad (14)$$

The collector spillage loss refers to the energy reflected by the heliostats that does not reach the heat absorber surface (after accounting for shading losses). In this context, we represent the energy received by the collector with the number of rays that reach the collector. Thus, based on the solar incidence angle, the average truncation efficiency can be obtained as follows:

$$\overline{\eta_{trune}} = \frac{1}{N} \sum_i^n \eta_{itrune} \quad (15)$$

Changes in the mirror's reflectivity can also affect the optical efficiency. However, since the reflectivity of the mirror is an inherent property, it can be set as a constant. Here, it is set with a reflectivity value of 0.92.

Considering all the above, the formula for calculating optical efficiency is shown as follows:

$$\eta = \eta_{at} \eta_{cos} \eta_{ref} \eta_{sb} \eta_{trune} \quad (16)$$

2.1.3. Thermal Output Power of the Heliostat Field

In optics, irradiance is the power of electromagnetic radiation incident on a surface per unit area. Radiant exitance is the power per unit area radiated from a surface, which in this context represents the solar radiation energy received per unit time in the direction perpendicular to the normal.

Based on the optical efficiency and normal direct irradiance, the total thermal output power of the heliostat field can be obtained:

$$E_{field} = DNI \cdot \sum_i^N A_i \eta_i \quad (17)$$

Furthermore, based on the total thermal output power of the heliostat field, the average output thermal power can be derived, with the calculation formula shown as follows:

$$\overline{E_{field}} = \frac{E_{field}}{N} \quad (18)$$

The formula for calculating the annual average thermal output power is shown in the following equation:

$$\overline{E_{Tfield}} = \frac{1}{60} \sum_k^{12} \sum_j^5 \overline{E_{jkfield}} \quad (19)$$

Where j represents the j-th moment and k represents the k-th month.

2.2. Grid Marking Method Based on Plane Projection Model Judgment Algorithm

Due to the difficulty in calculating the area of the shadow region in a heliostat field, this paper simplifies the conclusion of the topic by obtaining the projection efficiency of the heliostat through a grid standardization method. First, based on the division of the grid on the surface of the heliostat, the table center point is denoted as $P_{ij}(x_{ij}, y_{ij})$, where i,j represent the row and column of the center point, and the row and column spacing is known. A zero matrix E of $I \times J$ is established. Through projection, the intersection points of the projection edges with the heliostat, as well as the fixed points of the heliostat on the projected quadrilateral, are determined. These points, together with the boundary points of the heliostat, form an irregular region. The center points of the grids within this region are set to 1. The schematic diagram of the above judgment algorithm is shown in Figure 2.

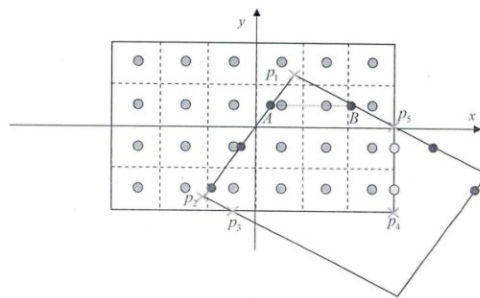


Figure 2: Schematic diagram of the judgment algorithm.

This type of method searches and determines as follows: First, by selecting the maximum value of the vertical coordinate from the aforementioned points and searching to the right, set it as 1. Stop when x_{i+1} exceeds the boundary value. Then, continue with the aforementioned steps after subtracting Δy from y_n , until y_n is less than or equal to 0. Finally, by calculating the number of 0s in the matrix divided by the number of grids, η_{sb} can be obtained.

By solving the aforementioned model, the optical distribution of the heliostat field can be obtained,

and the optical efficiency for different months is shown in Figure 3.

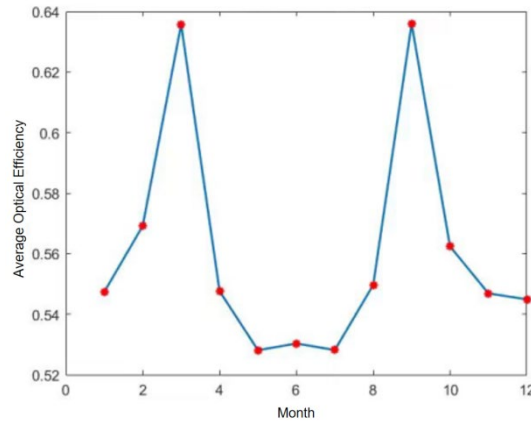


Figure 3: Average optical efficiency by month.

3. Optimization of Heliostat Field Layout

3.1. Establishment of EB Layout and Optimization Model

EB layout refers to the arrangement field formed by the distribution of heliostats under unobstructed conditions. The EB layout diagram is composed of different areas and rings. The initial layout of the mirrors can be established through basic parameters, with the adjacent heliostats in each area of the ring having the same spacing, as shown in the formula:

$$\Delta Az_{1,1} = \Delta Az_{2,1} = \dots = \Delta Az_{i,1} = A_{sf} \cdot SW \quad (20)$$

At this point, the spacing $\Delta Az_{i,k}$ between the areas of the mirror surfaces is related to the orientation angle and radius of the heliostats:

$$\Delta Az_{i,j} = 2R_{i,j} \sin(\Delta \alpha_{i,j}/2) \quad (21)$$

The orientation angle can also be calculated based on the adjacent spacing and ring radius of the first ring of each area.

$$\Delta \alpha_j = \arcsin(\Delta Az_{i,1}/(2R_{i,1})) \quad (22)$$

Here, it is assumed that the number of heliostats in the same ring of the mirror field is the same. Let $N_{bel,i}$ be the number of heliostats in each ring of the i -th area, then we have:

$$N_{bel,i} = 2\pi/\Delta \alpha_i \quad (23)$$

Using the aforementioned parameters, consider the dispersion of the radiation axis and, in the case of expanding the radius of the heliostat field, use A_{rlim} to limit the orientation spacing of the areas.

$$A_{rlim} = \frac{\Delta Az_{1,k}}{\Delta Az_{1,1}} = \frac{\Delta Az_{2,k}}{\Delta Az_{2,1}} = \frac{\Delta Az_{i,k}}{\Delta Az_{i,1}} \quad (24)$$

Additionally, based on geometric relationships, the size of the radial spacing satisfies the following formula:

$$\Delta R_{1,1} = \sqrt{(DM^2 - (\Delta Az_{1,1}/2)^2)} \quad (25)$$

Since the requirement is to maximize the annual average thermal output power per unit mirror area when the heliostat field reaches its rated power, the average thermal output power should be the objective, thereby obtaining the optimization model for this scenario.

The objective function is:

$$\arg \max \overline{E_{Field}} = \frac{1}{60} \sum_k^{12} \sum_j^5 \frac{E_{field}}{N \cdot A} \quad (26)$$

Where A represents the sum of the areas of all the heliostats in the field, and its calculation formula

is:

$$A = NA_i \quad (27)$$

Constraints are: $\overline{E_{field}} \geq 60$, $2 \leq \Delta h \leq 6$, $2 \leq \Delta l \leq 8$, $\Delta h \leq \Delta l$, $|d_{ij} - \Delta l| \geq 5, \frac{\Delta l}{2} \leq h_{HelioStat}$.

3.2. Particle Swarm Optimization (PSO)

Particle Swarm Optimization (PSO) is an evolutionary algorithm based on the concept of swarm intelligence. The idea is inspired by artificial life and evolutionary computation theories. It uses the experience of others as a basis for self-decision making, forming a fundamental concept of PSO. Here are the steps involved:

1) Initialization: Start by selecting particles that are closest to the extreme values and set their current positions as the best positions.

2) Evaluation: Assess each particle by calculating its fitness. If the fitness is higher than the current value, update the extreme values.

3) Particle Update: Update the position coordinates of each particle based on the current situation.

4) Termination Check: Determine whether to end the process. If a set number of iterations have been reached or a predetermined error threshold is met, stop the iteration. Otherwise, return to step 2.

Based on the aforementioned model, the annual average optical efficiency $\bar{\eta}$ of the heliostat field satisfies the following function:

$$\bar{\eta} = f(h_{tower}, \Delta h, \Delta l, x_i, y_i, \alpha_s, \gamma_s) \quad (28)$$

The aforementioned parameters are referred to as the heliostat field layout parameters. By specifying the EB layout, the number of layout parameters can be reduced, transforming the heliostat field layout parameters into the A_{rim} and $\Delta R_{1,1}$ within the EB layout, thereby simplifying the constraints. The simplified constraints are:

$$A_{rim} - \Delta l \geq 5 \quad (29)$$

Since the heliostats are arranged according to the EB (Edge of Bubble) layout, it is only necessary to assess the minimum values. It can be assumed that the distance between adjacent heliostats is greater than the width of the mirrors by at least 5 meters. Given that this is considered an EB layout, the shadowing rate η_{sb} is considered to be constant at 1. This simplifies the parameters in the objective function.

3.3. Solution of Heliostat Field Coordinates in EB Layout Model

Due to the complexity of determining decision variables and calculating the positions of the heliostat field in the ground coordinate system, this paper first solves the layout coordinates using a coordinate system centered on the receiver tube, and then converts them into heliostat field coordinates. The main steps are as follows:

Step 1: Determine whether the coordinates are within the same area and whether there is any shading between them to find if the minimum value ΔR_i is satisfied within the area at this time.

Step 2: By judging the maximum spacing of the restricted coordinate area, obtain the coordinates that meet the requirements at this time.

Step 3: Finally, convert polar coordinates to Cartesian coordinates through two coordinate transformations, and ultimately into heliostat field coordinates.

We obtain the average optical efficiency and output power on the 21st of each month as shown in Table 1. Specifically, the cosine efficiency heatmap of the heliostat field for January 21st is illustrated in Figure 4. The data presented in Table 1 reveals a pattern in the performance of the heliostat field throughout the year. Notably, the highest efficiencies are observed during the summer months, aligning with the period of peak solar insolation. Conversely, the winter months exhibit lower efficiencies, which can be attributed to the reduced solar altitude and increased atmospheric scattering. The heatmap provides insights into the distribution of efficiency across the field, highlighting areas of high and low performance. The color gradient effectively illustrates the variance, with warmer colors indicating higher efficiencies. This visual tool is instrumental in identifying potential areas for improvement

within the heliostat field layout.

Table 1: This caption has one line so it is centered.

Date	Average Optical Efficiency	Average Cosine Efficiency	Average Shadow Blocking Efficiency	Average Truncation Efficiency	Average Thermal Output Power per Unit Area of Mirror (KW/m ²)
1	0.715716146	0.705430182	0.985716146	0.929535977	0.779545121
2	0.692480126	0.725349193	0.952480126	0.924189185	0.679545121
3	0.691673029	0.745792192	0.991673029	0.920676568	0.678545121
4	0.700691669	0.764091785	0.999691669	0.918793367	0.764058491
5	0.699459241	0.774329281	0.989459241	0.919650469	0.7497035
6	0.649889513	0.777505394	0.999889513	0.920658688	0.757768136
7	0.629452055	0.77422013	0.999452055	0.919640663	0.749698268
8	0.651131821	0.763377476	0.981131821	0.918823937	0.615783984
9	0.70723647	0.744748641	0.98723647	0.920808075	0.757198881
10	0.637243207	0.722800503	0.987243207	0.924618313	0.574565486
11	0.665865259	0.703755084	0.975865259	0.930175631	0.574771643
12	0.663729171	0.696933872	0.983729171	0.933530209	0.554139862

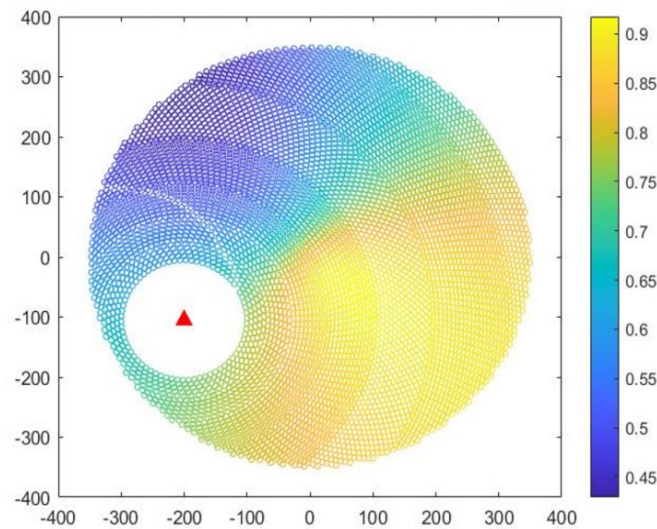


Figure 4: The cosine efficiency heatmap of the heliostat field.

The annual average optical efficiency and output power are shown in Table 2. It outlines the optimal design parameters derived from our model. These parameters include the absorber tower position coordinates, heliostat size, installation height, and the total number of heliostats and their collective area. The optimal parameters are crucial for achieving the highest possible efficiency and output power from the heliostat field. They serve as a guide for the physical layout and configuration of the heliostat field, ensuring that the system operates at peak performance.

Table 2: The annual average optical efficiency and output power.

Average Optical Efficiency	Average Cosine Efficiency	Average Shadow Blocking Efficiency	Average Truncation Efficiency	Average Thermal Output Power	Average Thermal Output Power per Unit Area of Mirror (KW/m ²)
0.6753	0.7495	0.9861	0.9407	0.686	137581

The optimal design parameters are shown in Table 3. These parameters include the absorber tower position coordinates, heliostat size, installation height, and the total number of heliostats and their collective area. The optimal parameters are crucial for achieving the highest possible efficiency and output power from the heliostat field. They serve as a guide for the physical layout and configuration of the heliostat field, ensuring that the system operates at peak performance.

Table 3: The annual average optical efficiency and output power.

Absorber Tower Position Coordinates	Heliostat Size	Heliostat Installation Height	Total Number of Heliostats	Total Heliostat Area
(17.69521,-182.8689)	6.061462	4.735483	5760	138240

4. Conclusions

The research conducted in this paper has successfully navigated the intricate process of optimizing the design of a heliostat field, leveraging the EB layout and Particle Swarm Optimization algorithm. Our study has demonstrated that through meticulous geometric analysis and the application of advanced computational methods, significant improvements can be achieved in the optical efficiency and thermal output power of heliostat fields. The seasonal performance analysis, underpinned by a comprehensive model that accounts for solar angles, atmospheric conditions, and DNI, has shed light on the variability in system efficiency, with a notable peak during the summer months. The EB layout, with its strategic arrangement of heliostats, has emerged as a pivotal strategy in minimizing shading and maximizing solar energy capture. The optimal design parameters, including the positioning of the absorber tower and the dimensions and installation height of the heliostats, are instrumental in fine-tuning the field's performance to its highest potential. The findings of this study not only contribute to the academic discourse on solar energy optimization but also hold practical relevance for the design and operation of solar thermal power plants. As we conclude, the implications of this research extend to the broader goal of enhancing the sustainability and economic viability of solar power generation, offering a roadmap for future advancements in the field.

References

- [1] Pfahl A, Coventry J, Röger M, et al. Progress in heliostat development[J]. *Solar Energy*, 2017, 152: 3-37.
- [2] Yerudkar A N, Kumar D, Dalvi V H, et al. Economically feasible solutions in concentrating solar power technology specifically for heliostats—A review[J]. *Renewable and Sustainable Energy Reviews*, 2024, 189: 113825.
- [3] Ali K, Jifeng S. Research on modeling simulation and optimal layout of heliostat field optical efficiency for Solar Power Tower Plant[J]. *Applied Solar Energy*, 2023, 59(6): 957-977.
- [4] Wang D, Tan D, Liu L. Particle swarm optimization algorithm: an overview[J]. *Soft computing*, 2018, 22(2): 387-408.
- [5] Mahboob K, Awais Q, Khan A, et al. Selection of Sensors for Heliostat of Concentrated Solar Thermal Tower Power Plant[J]. *Engineering Proceedings*, 2021, 12(1): 41.
- [6] Leonardi E, Pisani L. Analysis of Heliostats' Rotation Around the Normal Axis for Solar Tower Field Optimization[J]. *Journal of Solar Energy Engineering*, 2016, 138(3): 031007.